Synthesis of Waterborne Anticorrosive Coatings Based on The Incorporation of Phosphate Groups to Polyurethane-Acrylate Hybrids

Aitor Barquero,* Oihane Llorente, Daniela Minudri, María Paulis, and Jose Ramon Leiza*

In this work, solvent-free waterborne polyurethane-poly(meth)acrylate hybrid dispersions that can be used to formulate anticorrosive paints are synthesized. To achieve the anticorrosive protection, a phosphate containing polymerizable surfactant, Sipomer PAM 200 is incorporated to the hybrids. The presence of phosphate groups can produce an iron phosphate passivation layer to provide coatings with anticorrosive properties. These properties are tested in both mild and harsh corrosive environments. It is observed that when the films are dried at 60% relative humidity conditions, very poor anticorrosive protection is achieved because no phosphatization is obtained, but increasing the humidity to 85% during the drying step allows the formation of the passivation layer providing good anticorrosive properties.

1. Introduction

Corrosion in metal structures is a worldwide problem that affects the whole modern society and has a great impact in the global economy.[1–3] Mild steel is one of the most relevant materials and it is used in a broad range of different areas, such as construction, transport, utilities, and buildings. However, the metal structures are considerably affected by corrosion, leading to the degradation and/or frequent infrastructure maintenance, which causes great economic loss.[4] For that reason, many studies are focused

A. Barquero, O. Llorente, M. Paulis, J. R. Leiza
POLYMAT, Kimika Aplikatua saila, Kimika Fakultatea, Universidad del País Vasco/Euskal Herriko Unibertsitatea UPV/EHU
Joxe Mari Korta zentroa
Tolosa, hiribidea, 72, Donostia 20018, Spain
E-mail: aitor.barquero@ehu.eus; jrleiza@ehu.eus
D. Minudri
POLYMAT, Universidad del País Vasco/Euskal Herriko Unibertsitatea UPV/EHU
Joxe Mari Korta zentroa
Tolosa, hiribidea, 72, Donostia 20018, Spain

on improving metal substrates protection by the use of a coating against corrosion.

Corrosion is an electrochemical process that happens as a result of the presence of electrical potential differences.[4–7] When the surface gets in touch with water, oxidation reaction occurs in the anode with the formation of metal ions (Fe^{2+}) and free electrons, which in presence of dissolved oxygen and acidic media, will react in the cathode to generate other chemical species and eventually cause the formation of iron hydroxide or rust.

The main strategy to protect a steel structure from corrosion is to apply a protective coating to the surface, which will stop the corrosion agent from reaching the metal. The use of a protective coating that will stop corrosion will extend the durability of metal substrates, and therefore, reduce the maintenance and environmental cost.[8,9]

Typically, for less demanding applications, acrylic waterborne coatings are used. This type of coatings not only present excellent outdoor and alkali resistance, good compatibility with pigment and low cost, but also as they are synthetized and commercialized in waterborne media, they are an environmentally friendly solution.[10–12] However, the application range of these systems is sometimes limited, as their properties are not always competitive. On the one hand, the mechanical properties of waterborne coatings are limited due to the film formation paradox[13,14] that is, the necessity to have hard and scratch-resistant films with good mechanical properties, which means high glass transition temperature, combined with low minimum film formation temperature to obtain a film at room temperature.

On the other hand, there are specific challenges concerning anticorrosive waterborne coatings. One is the presence of surfactant in the binder; an essential component to ensure the stability of the polymer particles in waterborne polymeric dispersion, but that can migrate during the film formation process.[15,16] It can migrate toward air-coating or coating-substrate interfaces, it can form hydrophilic aggregates inside the film or it can be trapped at the particle/particle boundaries. In any case, film properties such as water resistance are damaged. The second challenge is the formation of flash rust.[17,18] This phenomenon is very common when metallic substrates are in direct contact with water, and consists on the rapid formation of a thin oxidation layer that is formed within minutes of contact.

For these reasons, acrylic waterborne coatings are still not suitable for very demanding applications, such as marine

ADVANCED
SCIENCE NEWS

www.advancedsciencenews.com

acro-
molecular
Reaction Engineering
www.mre-journal.de

environments (for ships, offshore mills, and other types of large infrastructures). Thus, the market for these applications is dominated by solventborne epoxy and polyurethane-based coatings.[19–21] Admittedly, the properties of these coatings are excellent, but are not environmentally sustainable products, as large amounts of volatile organic compounds are emitted to the atmosphere. That is why there is still the necessity of developing waterborne systems that can compete with the solventborne products.

In this work, we explore the possibility of creating waterborne polyurethane-acrylic hybrid dispersions that contain phosphate groups on the surface of the particles. If the phosphate groups are located in the surface of the particles, they can react with the iron to form an iron phosphate passivation layer. Therefore, our focus was on exploring different possibilities to incorporate the phosphate functionalities into the hybrid polymer. There are different methods to synthetize polyurethane-acrylic dispersions, such as miniemulsion[22,23] seeded emulsion polymerization[24,25] or simultaneous polyaddition and free-radical polymerization.[26,27] For this work, a solvent-free process that was already developed on previous works has been considered.[28,29] The advantage of this method is that it does not require the use of high temperatures, solvents, or additional miniemulsification. The synthesis is done in two steps: first, the polyurethane (PU) prepolymer containing carboxylate groups is synthetized using the acrylic monomers as solvent. Then the solution is dispersed in water (using the acid groups as stabilizer) and the acrylic monomers are polymerized by emulsion polymerization in batch. It is noteworthy that for the strategy followed in this work, the polyurethane does not contain any reactive vinyl group and the acrylic monomers did not contain any hydroxyl functionality, and therefore, the PU and acrylic phases are not chemically bonded.

In the first part of the work, we present different attempts of incorporate phosphate groups in the polyurethane part. The idea was to substitute the carboxylic groups by phosphate groups, so the polyurethane could still function as the stabilizer of the system, but with the additional capacity of corrosion protection. Some of the work was inspired by Kakati et al.[30] that showed that β-glycerol phosphate can be used as ionic diol monomer. Other trials were inspired by Mequanint and coworkers, using 2-phosphonobutane-1,2,4-tricarboxylic acid to synthetize phosphate containing macrodiols.[31–33] In both cases, the processes developed by the authors involved the use of organic solvents, so we attempted to adopt them to our solvent-free process. However, the challenges that arouse these systems could not be overcome, and we did not succeed in achieving a suitable formulation. Nonetheless, we consider that reporting these results can be useful for future researchers and therefore worth to be reported.

Because the first strategy did not succeed, in the second part of this work, we explore the use of Sipomer PAM 200 as comonomer during the polymerization of the acrylic monomers (see the structure in Figure SI.1 in the Supporting Information). Recent works have shown that the use of this polymerizable surfactant (Sipomer PAM 200) can provide (meth)acrylate-based waterborne dispersions with excellent anticorrosive properties.[34–36] Under the right drying conditions, the formation of the iron phosphate layer is faster than the formation of flash rust, there-

fore avoiding the phenomena.[36] Moreover, as the Sipomer PAM 200 is a polymerizable surfactant, it is covalently bonded to the polymer, avoiding the surfactant migration and the problems related.

For an optimal corrosion protection, phosphate groups should be on the surface of the particles in order to obtain the best formation of the anticorrosive passivation layer, so they can easily react with the iron on the steel surface. It has already been shown that the most efficient incorporation of polymerizable surfactant is obtained by semibatch processes.[37,38] Therefore, herein we will explore different alternatives on the second step of the synthesis of the hybrids (the polymerization of the acrylic monomers) to ensure the adequate incorporation of the Sipomer PAM 200 and provide the best performance.

2. Experimental Section

As the different attempts to incorporate the phosphate functionality in polyurethane phase were unsuccessful, the materials for that Section (3.1) are presented in the Supporting Information. In this section, the experimental details of the results reported in Section 3.2 (where the phosphate is incorporated in the acrylic phase) of this work are presented.

2.1. Materials

Isophorone diisocianate (IPDI), polypropylene glycol (PPG, M_n = 2000 g mol^{-1}), dimethylol propionic acid (DMPA), butanediol (BDO), triethylamine (TEA), hexamethylene diamine (HMDA), dibutyltin dilaurate (DBTDL), and potassium persulfate (KPS) were purchased in Sigma-Aldrich. Methyl methacrylate (MMA) and n-butyl acrylate (BA) were purchased from Quimidroga. Sipomer PAM 200 was kindly supplied by Solvay. Deionized water was used in all reactions. Mild steel AS1020 substrates (medium carbon steel with 0.5% of C) were purchased from Urduri S.L. (Spain). High purity NaCl (Corrosalt, Ascott-Analytical) was used for the corrosion tests. The tetrahydrofuran (THF) used for soxhlet extraction was synthesis grade (Fisher Scientific) and the THF for the size exclusion chromatography (SEC) analysis was HPLC grade (Scharlau).

2.2. Synthesis

The synthesis of the hybrids was a solvent-free process where the polymerization of the polyurethane and polyacrylate phases were carried out in separate steps. A 250 mL jacketed reactor was used, equipped with nitrogen inlet, condenser, sampling device, and mechanical turbine stirrer rotating at 200 rpm. In the first step, a polyurethane prepolymer with excess NCO groups was synthetized using 70 % of the total acrylic monomers as solvent. First, the IPDI was mixed with PPG, DMPA, DBTDL, and the acrylic monomer mixture. Note that all components with the exception of DMPA are soluble in the acrylics. The mixture was heated to 70 °C and left to react for 5 h. After that, all the DMPA had reacted and a homogeneous mixture was obtained. The chain

Table 1. Formulation and step-by-step process for the synthesis of the PU prepolymer.

Step	Ingredient	Relative mol	Weight [g]	Temperature [°C]	Time
1. PU prepolymer	DMPA	0.37	4.31	70	5 h
	PPG	0.19	33.04		
	IPDI	1	19.33		
	DBTDL	—	0.20		
	Acrylics[a]	—	21.00		
2. Chain extension	BDO	0.07	0.55	70	2 h
	Acrylics[a]	—	8.4		
3. Cooling	Acrylics[a]	—	8.4	25	
4. Neutralization	TEA	0.39	3.4	25	45 min
	Acrylics[a]	—	4.2		

[a] Acrylic monomer mixture composition: MMA and BA in a 50/50 weight ratio.

Table 2. Formulation used for the free-radical polymerization step.

Ingredient	Weight [g]
PUD	40
Acrylics	3.14
Sipomer PAM 200	0.209
KPS	0.105
Water	12.00

extension step was carried out by adding the BDO dissolved in some of the acrylics as a shot, and left to react for two more hours. Then, the mixture was cooled down to 25 °C, and an additional amount of the acrylic monomers was added to reduce the viscosity of the mixture. At the end, TEA was added to neutralize the acid groups of DMPA. **Table 1** gives a step-by-step description of the PU prepolymer process and formulation used.

For the dispersion of the PU prepolymer, the same reactor was used. At room temperature, 90 mL of water were charged to the reactor. 60 g of the PU prepolymer were added dropwise using a syringe under stirring at 300 rpm. After all the PU prepolymer was dispersed, HMDA (3.112 g) dissolved in water (4.2 g) was added dropwise for the final chain extension. It was left stirring at room temperature and 200 rpm for 1 h.

The same batch of polyurethane dispersion (PUD) and formulation were used for all reactions. The difference between different runs laid on the strategy that was used for the polymerization of the acrylic monomers and particularly the addition of the Sipomer PAM 200 (phosphate containing monomer) to the reactor. All reactions were carried out at 70 °C and a shot of an aqueous solution of KPS (0.5 wt% with respect to the acrylics) was used as initiator. The same reactor as for the PU prepolymer synthesis was used, with a turbine stirrer at 200 rpm. **Table 2** shows the general formulation used for the free-radical polymerization step, and **Table 3** describes the different feeding strategies of the monomers. The final product was a 40% S.C. latex with a 50/50 wt% ratio between the polyurethane and polyacrylate phases.

2.3. Characterization

The final solids content (S.C.) of the hybrid latexes was measured gravimetrically by weighting an aliquot of the latex before and after it was dried.

Fourier Transform Infrared Spectroscopy (FTIR) was used to confirm the full conversion of isocyanate groups (at 2270 cm^{-1}) after the chain extension step. Bruker Alpha-P spectrometer was used to obtain the spectra by attenuated total reflectance technique.

The z-average particle diameter was measured by dynamic light scattering in a Nano ZS Zetasizer from Malvern Instruments. The samples were prepared diluting a drop of latex in 1 mL of doubly deionized water. The analyses were carried out twice at 25 °C and an average value is reported. The z-potential of the particles was measured using the same sample in the same equipment.

The molar mass distribution of the polymers was measured by SEC. The samples were first dried in an oven at 65 °C and then redissolved in THF to achieve a concentration of about 3 mg mL^{-1}. The solutions were filtered with a polyamide filter (pore size = 0.45 μm) before they were injected into the SEC instrument. The SEC instrument consisted of an autosampler (Waters 717 plus), a pump (LC-20, Shimadzu), three columns in series (Styragel HR2, HR4, and HR6 with a pore size from 10^2 to 10^6 Å) and a differential refractometer (Waters 2410) as detector. The flow rate of THF through the columns was 1 mL min^{-1}. The reported molar masses are referred to polystyrene standards.

The gel content is defined as the polymer fraction that is not soluble in tetrahydrofuran (THF), and it was determined by soxhlet extraction. The extraction was carried out using glass fiber pads as backing. The glass fiber pad (CEM) was weighted (W_1). A few drops of latex were put on the fiber glass pad and dried in an oven at 65 °C overnight. The fiber glass pad with the polymer was weighted again (W_2) before performing a continuous extraction with THF under reflux in the soxhlet for 24 h. The fiber glass pad was dried in an oven at 65 °C overnight and weighted (W_3). The gel content was calculated with Equation (1)

$$\text{Get } content\ (\%) = \frac{(W_3 - W_1)}{(W_2 - W_1)} \times 100\ \text{k} \tag{1}$$

The water uptake measurements were made immersing dried polymer films in doubly deionized water and measuring the gain of weight over time. After 14 days of immersion, the films were dried and weighted again to measure the weight loss. The water uptake and weight loss were measured using Equations (2) and (3), respectively

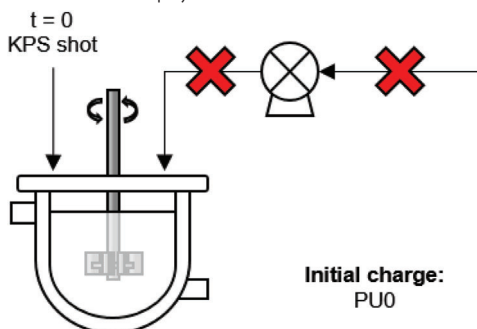$$\text{Water uptake (t) }(\%) = \frac{W_{wet}(t) - W_{Dry, after}}{W_{Dry, after}} \times 100 \tag{2}$$

$$\text{Weight loss }(\%) = \frac{W_{Dry, before} - W_{Dry, after}}{W_{Dry, before}} \times 100 \tag{3}$$

were W_{Wet} is the weight of the film swollen with water at each time, $W_{Dry,before}$ is the weight of the dry film before the experiment, and $W_{Dry,after}$ is the weight of the dry film after the experiment.

ADVANCED
SCIENCE NEWS
www.advancedsciencenews.com

[M]acro-
olecular
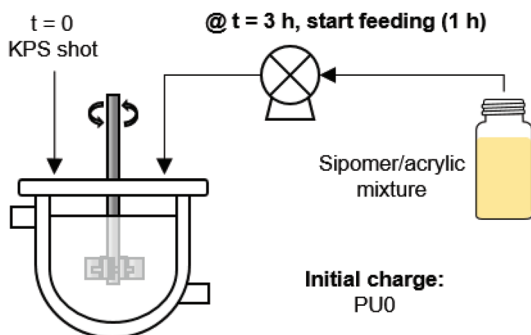Reaction Engineering
www.mre-journal.de

Table 3. Description of the different monomer feeding strategies used for the free-radical polymerization step.

PU0: The polyurethane dispersion swollen with acrylic monomers before any free-radical polymerization

PU1: Blank reaction without adding Sipomer PAM 200, the acrylic monomers were polymerized in batch.

PU2: The Sipomer PAM 200 dissolved in the remaining acrylics was fed over 1 h during the polymerization of the acrylics in the PUD.
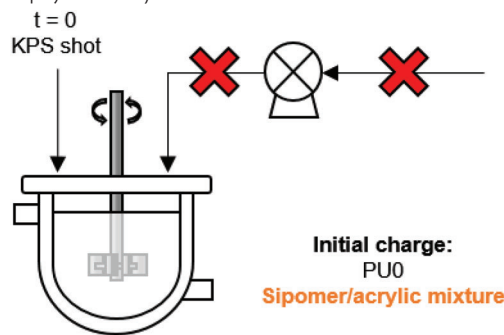
PU3: The acrylics in the PUD were polymerized for 3 h and after that, the Sipomer PAM 200 (dissolved in the remaining acrylics) was fed to the reactor over 1 h with an additional shot of initiator solution.
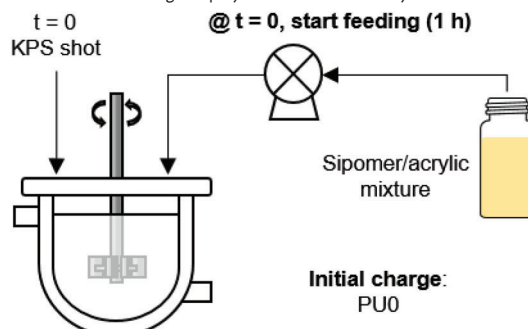
PU4: All the remaining acrylic monomer and Sipomer PAM were added to the reactor before the shot of initiator (batch polymerization).

The water static contact angle was measured on a 60 µm thick film casted onto the steel surface and left to dry for 24 h at 23 ± 2 °C and 60 ± 5% R.H. The measurement was carried out in a Contact Angle System OCA (Dataphysics) equipment, taking an average from five measurements.

In order to evaluate the corrosion protection of the synthetized latexes three different tests were performed. For all tests, the samples were prepared by directly coating the steel substrate with the latex, using a film applicator of 120 µm wet thickness and drying them at 23 ± 2 °C and 60 ± 5% R.H. or at 23 ± 2 °C and 85 ± 5% R.H. for 24 h. The only treatment done to the substrates before the coating was to clean them with acetone to degrease them. The dry film thickness was around 50 µm.

Electrochemical impedance spectroscopy (EIS) measures the impedance of the coating/metal interface by applying an AC voltage to a coated test specimen. For that, a three-electrode cell was used: Ag/AgCl saturated with KCl was used as reference electrode, platinum mesh as counter electrode and the different coatings (11 mm of diameter) as working electrode. All the tests were immersed in 3.5 wt% NaCl solution at room temperature for 24 h using a BioLogic VMP3 multichannel potentiostat (Biologic, Seyssinet-Pariset, France) combined with EC Lab V10.44 software and measurements were performed every hour over a frequency range from 100 kHz to 10 mHz with 6 points per decade and a sinusoidal amplitude of 10 mV.
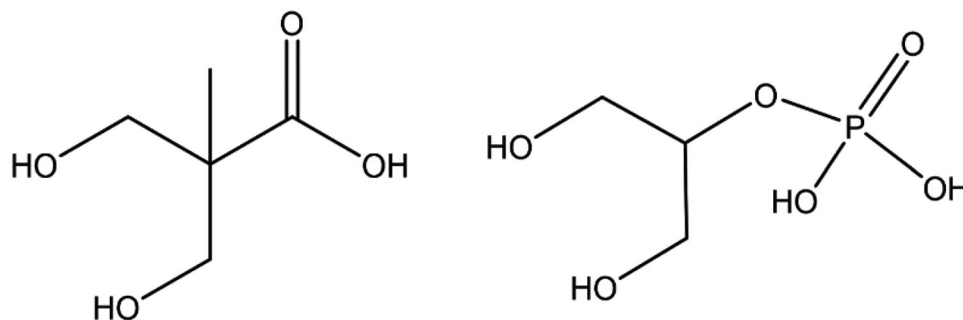
Anticorrosion protection was evaluated in both mild and harsh corrosive environments. For mild environment corrosion tests were performed by placing a drop of NaCl solution (5 mM) on top of the film and monitoring and visually evaluating the development of the corrosion over 24 h. Moreover, an additional test was performed in the same sample and under the same conditions but with an artificial scratch on the film, that would expose the metal. Figure 8 (in Section 3.2) shows a picture of the samples.

Salt spray measurements were carried out as harsh environments corrosive tests exposing mentioned coating to harsh corrosive conditions (5 wt% NaCl salt fog, ASTM B117 standard) using a salt spray chamber (Neurtek SC500). 3M vinyl tape 471 was used to prevent the starting of the corrosion in the uncoated corners of the substrates. Visual evaluation was done to assess coatings efficiency against corrosion.

3. Results and Discussion

3.1. Incorporation of Phosphate Groups in the Polyurethane

The first overall strategy to incorporate the phosphate functionality to the hybrid nanoparticles would be to incorporate it through the polyurethane phase. As advanced before, this strategy was not successful, but the results were interesting and are briefly discussed here regardless.

**ADVANCED
SCIENCE NEWS**

www.advancedsciencenews.com

**[M]acro-
molecular
Reaction Engineering**

www.mre-journal.de

Figure 1. Chemical structure of dimethylol propionic acid (DMPA, left) and β-glycerol phosphate (right).

The first approach was the straightforward substitution of the acid groups in the prepolymer by phosphate groups.[30] Carboxylic acid groups are incorporated using an acid diol such as dimethylol propionic acid (DMPA), so this component was substituted by a phosphate diol (β-glycerol phosphate). Both molecules have very similar structures, as shown in **Figure 1**, but bear different ionic groups.

B-glycerol phosphate is commercialized in its disodium salt form, therefore, before any reaction was carried out, an ion exchange resin (Dowex Marathon MSC hydrogen, Sigma-Aldrich) was used to obtain the diol. The water was removed by drying the solution in an oven at 65 °C overnight first, and by freeze-drying after. At the end of the process, a viscous liquid was obtained.[30]

The synthesis of the PU prepolymer was carried out following the process described in Section 2.2 and Table 1, just substituting the DMPA by β-glycerol phosphate in mole basis. The first drawback was that β-glycerol phosphate was not soluble in the monomer mixture. Nonetheless, initially this was not too concerning, as the DMPA cannot dissolve in the acrylic monomer mixture either, and the synthesis of the PU prepolymer is successful regardless. However, the prepolymer synthesis with β-glycerol phosphate did not produce the desired result. During the prepolymer synthesis, a precipitate was formed, seemingly the phosphate containing PU prepolymer, which was not soluble in the acrylics. The heterogeneous mixture could not be dispersed to produce particles, so it was not possible to produce the polyurethane dispersion.

When the β-glycerol phosphate was used in its disodium salt form, not only the PU precipitated, but it precipitated as an insoluble foam-like solid. Gravimetrically it was confirmed that all acrylic monomers remained unreacted, so the most likely reason for this was the reaction happening between the phosphate groups with the isocyanate.[39] crosslinking the prepolymer and making it unusable for this application.

The last attempt with β-glycerol phosphate as diol was done by mixing the protonated form with 2 mol equivalent of triethylamine, in an attempt to obtain a salt that would be more soluble in the acrylic monomers and less reactive with the isocyanate. This was not achieved, as β-glycerol phosphate and triethylamine did not mix.

β-glycerol phosphate disodium salt was used one more time, as chain extender in the chain extension step after the PU prepolymer was dispersed. For this trial, the PU dispersion was prepared as described in Section 2, but in the chain extension step, hexamethylene diamine was substituted by the β-glycerol phos-

phate disodium salt. This caused the coagulation of the system, likely due to increased ionic strength, and therefore this route was abandoned.
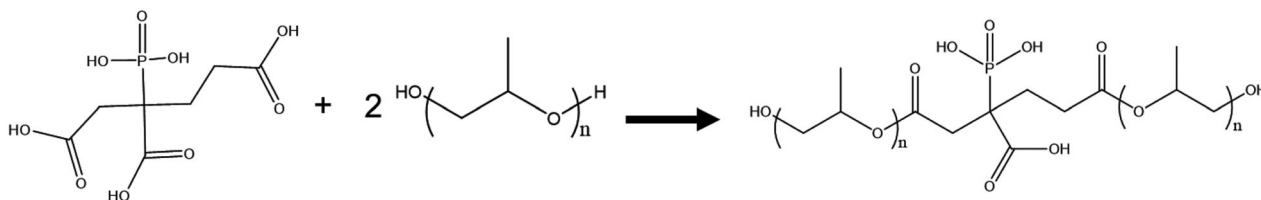
To improve the solubility of the phosphate groups in the acrylic monomers, it was decided to incorporate the phosphate groups through the macrodiol. Two different phosphate macrodiols were synthetized: one based on polypropylene glycol and a polyester diol.

The polypropylene glycol-based phosphate macrodiol was synthetized using polypropylene glycol ($M_n = 1000$ g mol^{-1}) and 2-phosphonobutane-1,2,4-tricarboxylic acid (2PBTA 50% aqueous solution, TCI). The esterification was carried out at 120 °C, with a 2:1 PPG/PBTA ratio and under nitrogen flow to promote the evaporation of water (see **Figure 2** for the reaction scheme).

This strategy was partially successful. It was possible to obtain the desired macrodiol (confirmed by MALDI-TOF experiments) and it was soluble in the acrylic monomers, but during the synthesis of the PU prepolymer, the solution formed a gel. It was possible to prevent the gelification of the solution by reducing the amount of phosphate macrodiol, but in return, the amount of ionic groups in the PU prepolymer was low. As a result, when the PU was dispersed and chain extended the final latex had a very poor stability. Nonetheless, it was possible to polymerize the acrylic monomers without having a massive coagulation. **Figure 3** shows a picture of the latex, a self-standing dried film, and the film casted on the steel substrate used for the corrosion tests.

As observed, neither the latex nor the film (dried in a silicone mold) were homogeneous. Moreover, because of the heterogeneity of the dispersion, when the film was casted in the steel plate, the coaguli were all deposited in one area of the substrate. Therefore, when the corrosion resistance test was carried out, both the "coagulum area" (on top) and the "non coagulum area" (on bottom) were tested. The performance of the corrosion test, presented in **Figure 4**, was relatively good (considering the quality of the coating), as after 24 h of exposure to the NaCl solution the corrosion did not significantly expand from the defect. For this reason, although this attempt was not considered successful, this method is promising.

The polyester route was much less successful. Inspired by Mequanint et al.[31–33] polyesters terminated in OH groups were synthetized using 2-phosphonobutane-1,2,4-tricarboxylic acid, adipic acid, and 1,4-butanediol at two different chain lengths. However, after purification, the polyesters could not be dissolved in the acrylic monomer mixture. In addition to the monomers that were used in the previous section (methyl methacrylate

ADVANCED
SCIENCE NEWS
www.advancedsciencenews.com

[M] acro-molecular
Reaction Engineering
www.mre-journal.de

Figure 2. Reaction scheme for the synthesis of the phosphate macrodiol from polypropylene glycol.

Figure 3. Picture of the latex (left), self-standing film (middle), and a film on the steel substrate of the PU/acrylic hybrid obtained using a phosphate macrodiol in the synthesis of the PU prepolymer.

and butyl acrylate) other monomers such as styrene, isobornyl methacrylate, and vinyl acetate were tried, but the polyesters did not dissolve in any. Thus, this route was not further explored.

3.2. Incorporation of Phosphate Groups in the Acrylics via Sipomer PAM 200

3.2.1. Synthesis of the Latexes and Characterization

The second strategy for the incorporation of phosphate functionality to the hybrid dispersions was through copolymerization with Sipomer PAM 200, during the free-radical polymerization

step. In this case, all the reactions that were tried produced stable dispersions. Before studying the anticorrosive properties of the different coatings, a general characterization of the latexes (including the polyurethane dispersion, PU0) was carried out, as presented in **Table 4**. Moreover, **Figure 5** shows the FTIR spectra of PU0 after evaporating the water and the acrylic monomers. It can be observed that full conversion of the NCO groups was achieved due to the absence of any peak at 2270 cm^{-1}.

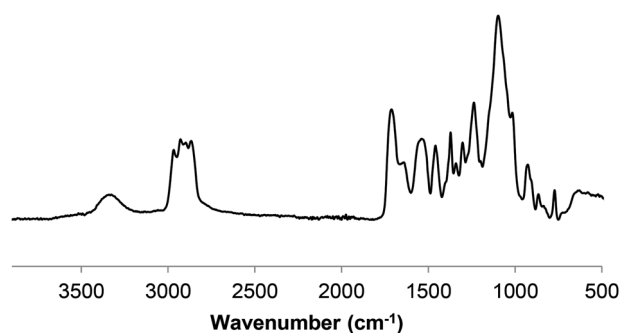As presented in Table 4, there are not significant differences in the properties of the final hybrid latexes. The solids content and final particle size of PU1 (reference without Sipomer) is slightly lower than for the rest of the hybrids, but this is because for this run no additional acrylic monomers were fed for the second
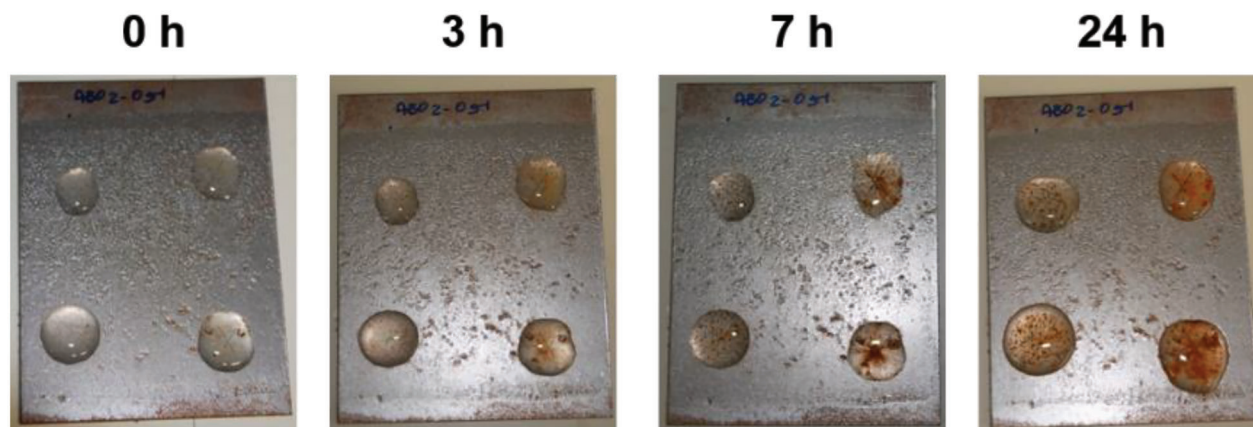
Figure 4. Time evolution of the steel substrate coated with the hybrid containing the phosphate macrodiol during the corrosion test.

2300015 (6 of 13)

**ADVANCED
SCIENCE NEWS**

www.advancedsciencenews.com

**Macro-
molecular
Reaction Engineering**

www.mre-journal.de

Table 4. Characterization of the polyurethane prepolymer dispersion after chain extension (PU0) and polyurethane-polyacrylate hybrids (PU1-4) at the end of the polymerization.

	S.C. [%]	dp [nm]	z-potential [mV]	Gel content [%]	M_w [kg mol^{-1}]	Đ
PU0	28	66 ± 0	−52 ± 2	0.1 ± 0.0	29.7	1.54
PU1	35	76 ± 0	−50 ± 3	0.4 ± 0.3	91.6	3.17
PU2	39	102 ± 0	−50 ± 0	0.2 ± 0.0	77.2	2.75
PU3	40	98 ± 1	−53 ± 0	1.0 ± 0.1	82.9	3.15
PU4	40	122 ± 1	−50 ± 1	3.8 ± 0.3	57.3	2.49

Table 5. Water sensitivity properties of the polyurethane-polyacrylate hybrids films.

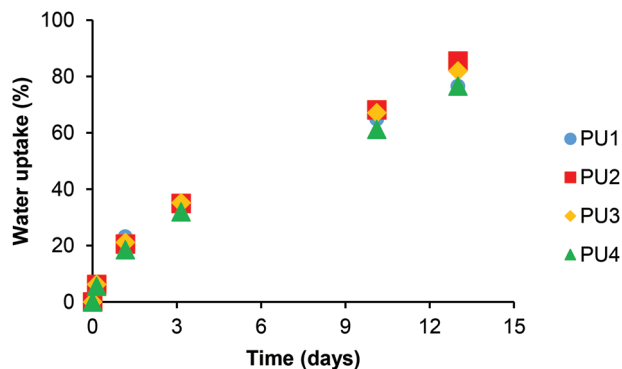|	14 days water uptake [%]	Weight loss [%]	Contact angle [°]
PU1	76	2.3	74 ± 3
PU2	85	2.2	71 ± 2
PU3	82	2.2	76 ± 1
PU4	77	2.4	74 ± 1

Figure 5. Transmission FTIR spectra at the end of the reaction of the polyurethane dispersion (PU0).

polymerization step. The z-potential of the hybrid latexes is very similar to the one of the polyurethane dispersion (PU0), so no conclusion can be drawn regarding the incorporation of Sipomer Pam 200 to the surface of the particles. The molar masses are low for emulsion polymerization (especially when negligible gel was measured), likely due to transfer reactions to different components in the formulation, such as the triethylamine.[40]

The water sensitivity of the polymer films was evaluated by means of water uptake and static contact angle measurements. **Figure 6** presents the time evolution of the water uptake, and **Table 5** the final water uptake after 14 days, the weight loss after the experiment and the contact angle.

As observed, very similar water resistance is obtained for all films. The biggest differences can be found in the water uptake, where PU1 and PU4 show a slightly better performance. How-

ever, it is not easy to correlate the synthesis strategy with these results. The weight loss after the water uptake experiments are very similar (including the sample without Sipomer), which shows that the addition of Sipomer does not significantly promote the formation of hydrophilic water-soluble species, no matter the addition method. Last, very similar contact angles were obtained for all films.

3.2.2. Corrosion Resistance Tests

The anticorrosive properties of the films were tested. Before presenting the corrosion test results, **Figure 7** shows the steel substrates coated with the different hybrid latexes and dried at 23 ± 2 °C and 60 ± 5% R.H. for 24 h. In the substrate coated with PU1 (with no Sipomer) some corroded and nonhomogeneous dots are formed, while the rest of the substrates show clear and uniform coatings, with no visible defects or flash rust. However, due to the lack of color there is also no indication of phosphatization.[35] Iron phosphate has a characteristic yellow stain in the metal surface that is not present in the samples presented in Figure 7, so visual evaluation cannot confirm the formation of the passivation layer. Nonetheless, it has also been reported before that films with no yellow color show evidence of phosphatization and excellent anticorrosive properties,[34] so the corrosion tests were carried out regardless of the color.

Figure 8 shows the result of the corrosion test. To ease the comparison, only selected timeframes where differences are noticeable are presented.

The corrosion test shows the development of corrosion in a sample exposed to a mild corrosive environment (5 mm NaCl aqueous solution) with (top drop) and without (bottom drop) an artificial defect (scratch). As expected, the area with the scratch starts to corrode earlier than the area without defect. Namely, the area without defect only shows corrosion on the 24 h picture. It is noteworthy, however, that the specimen coated with PU1 shows no sign of corrosion after 24 h of experiment in the nonscratched area.

Regarding the area with the defect, for the first 3 h, no corrosion effect can be observed. At 5 h, however, the first signs of corrosion appear in PU1, and especially in PU3. This trend is more evident at 7.5 h, when a very clear brown stain appears in PU3. The brown color is a bit darker in PU1, and the first signs of corrosion appear in PU2. Interestingly, PU4 does not show any change in the color. After 24 h of experiment, all samples are completely corroded, and it is difficult to make any clear comparison. Nonetheless, anticorrosion protection was not achieved in these samples.
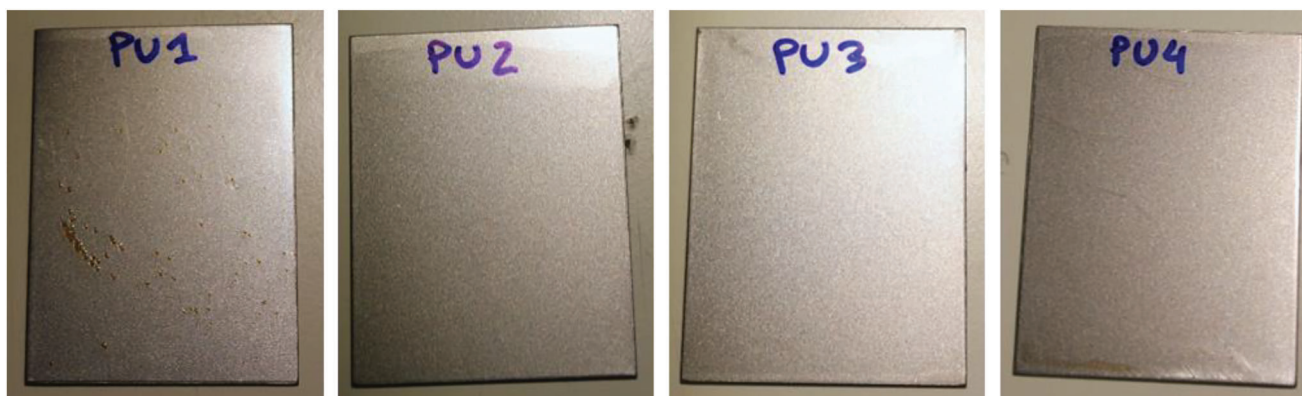

Figure 6. Time evolution of the water uptake of the PU/PA hybrid films.

Figure 7. Steel substrates coated with PU1, PU2, PU3, and PU4 dried at 23 ± 2 °C and 60 ± 5% R.H.
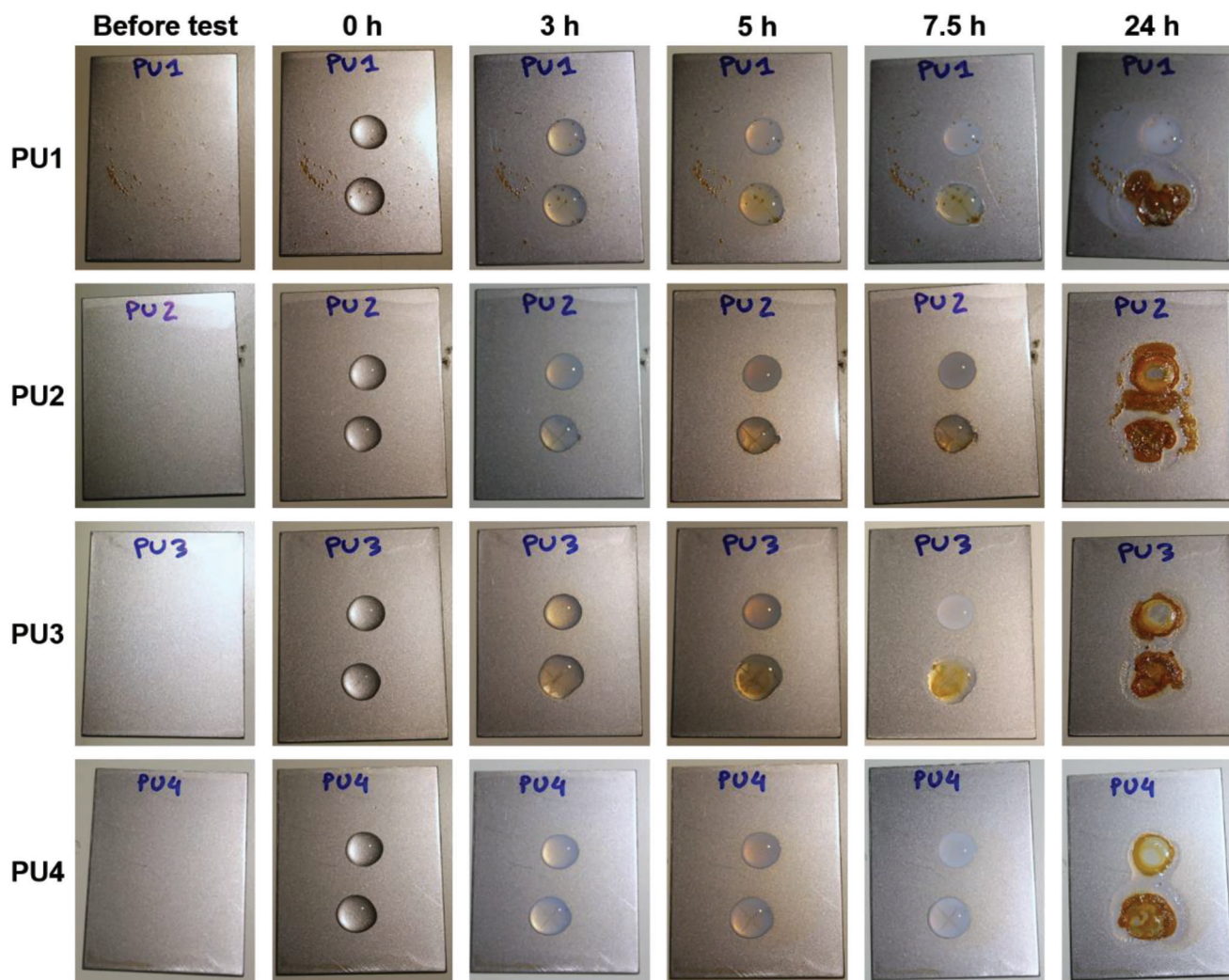
Figure 8. Time evolution of the coated steel substrates during the corrosion test.

**ADVANCED
SCIENCE NEWS**

www.advancedsciencenews.com

**[M]acro-
olecular
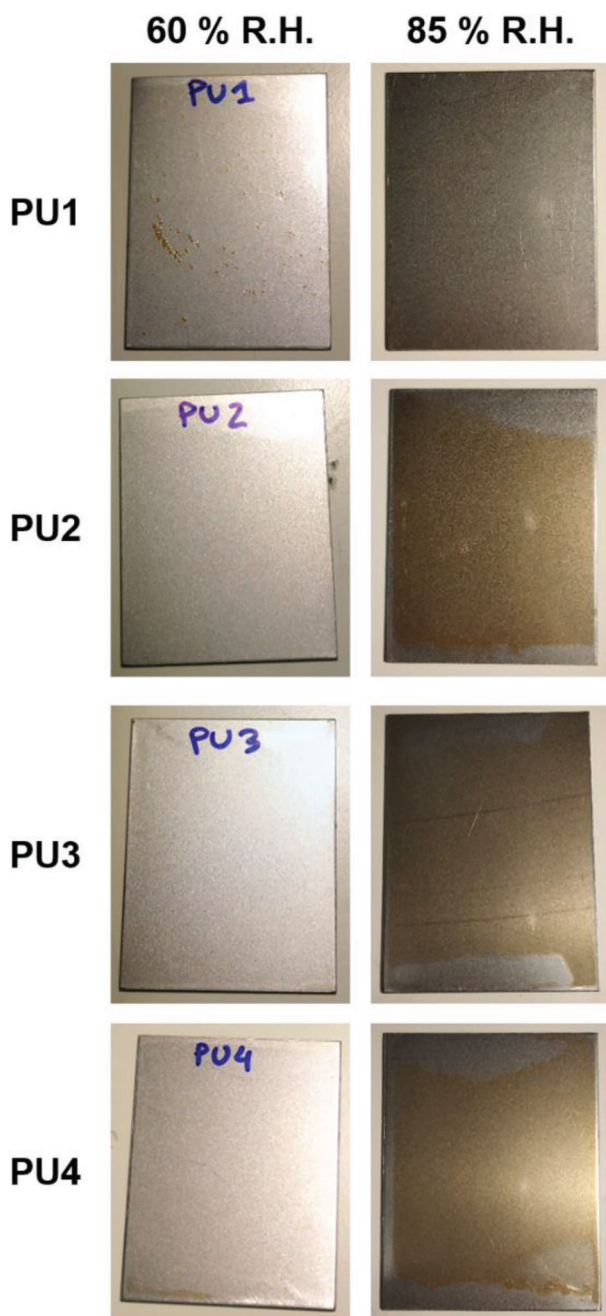Reaction Engineering**

www.mre-journal.de
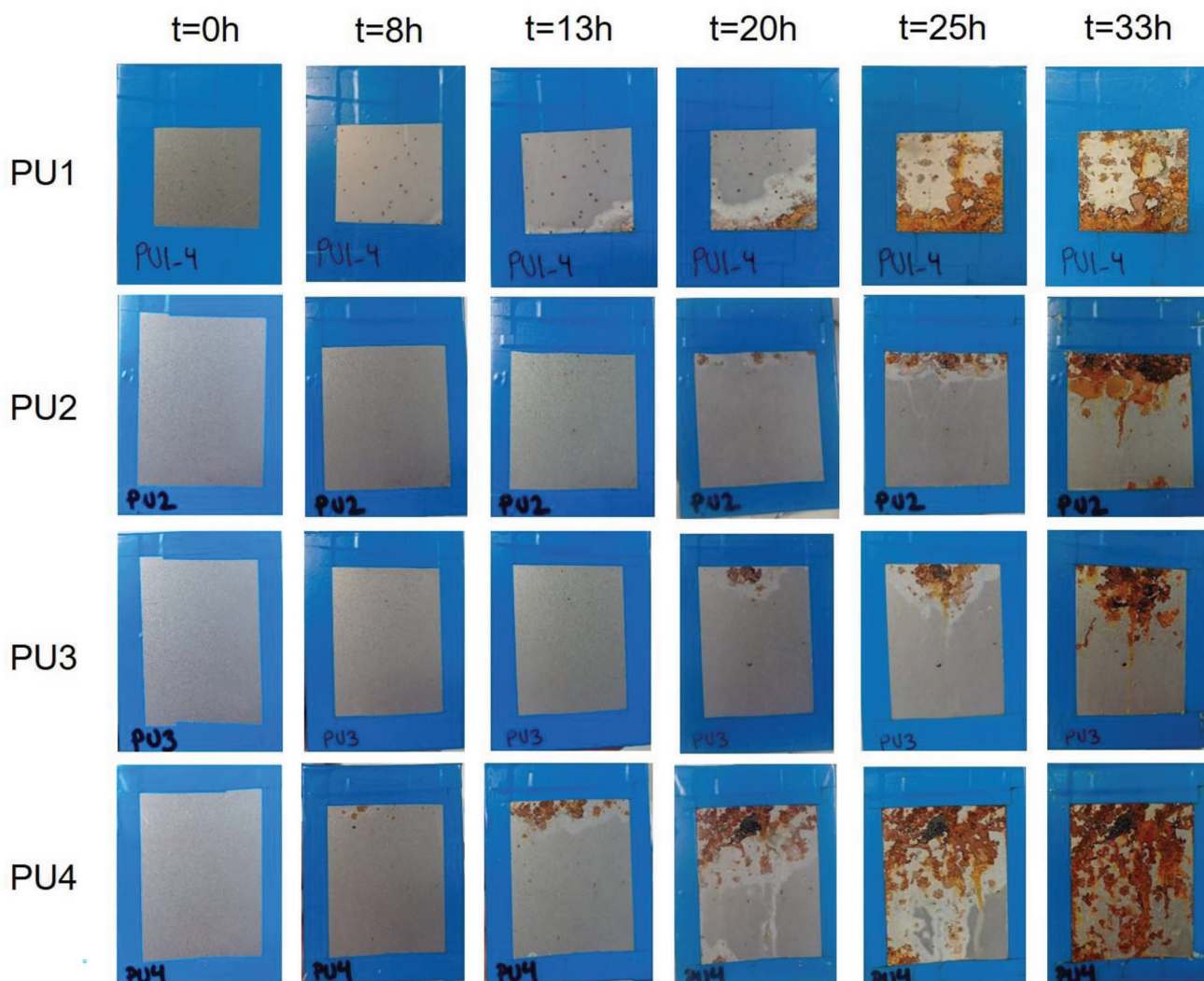
Figure 9. Results of salt spray test of PU-acrylic hybrid systems after different hours of exposure to 5 wt% NaCl salty fog.

Finally, **Figure 9** shows steel substrates coated with PUs at different salt spray exposure times to 5 wt% NaCl salty fog.

As discussed at the beginning of this section, at time zero PU1 shows rust dots, while the others coatings appear to be homogeneous. All samples showed a similar trend; a failure happens in a position of the coating, and then the corrosion propagates to the rest of the sample. Therefore, the main difference between samples is the time at which the initial failure starts. The first samples to fail are PU1 (slightly, in the bottom right corner) and PU4 (on top of the exposed area), at 8 h. PU2 and PU3 start to show rust at 20 h. In any case, none of the synthetized and applied coatings was able to withstand 24 h of salt spray, which indicates that an effective corrosion protection was not achieved. Once again, these results show that corrosion protection was not achieved (particularly if they are compared to those reported by Chimenti et al.[36,41] where an acrylic coating could resist for at least 400 h).

3.2.3. Improving Anticorrosive Properties by Promoting the Phosphatization

Results presented in Section 3.2 show that the anticorrosive properties of the synthetized coatings are very underwhelming. At the beginning the lack of yellow color that evidences the formation of the phosphatization layer was not considered crucial, however, due to the lack of anticorrosion protection of these coatings, this idea was revisited. Chimenti et al. already showed that the drying conditions were of extreme importance for the proper formation of the iron phosphate[36] At the same temperature, increasing the relative humidity increases the drying time. They observed that for their system 23 °C, 60% R.H. were ideal temperature and humidity conditions, and that lowering the humidity (increasing the drying rate, and decreasing the drying time) would not allow enough time to form the passivation layer. Thus, the drying humidity of the coatings was increased from 60% to 85% R.H.,

**ADVANCED
SCIENCE NEWS**

www.advancedsciencenews.com

**[M]acro-
molecular
Reaction Engineering**

www.mre-journal.de

Figure 10. Effect of drying conditions (relative humidity) on the formation of the phosphatization layer in PU-acrylic hybrids. Films were dried at 23 °C.

in an attempt to enhance the formation of iron phosphate. Indeed, as presented in **Figure 10**, when the relative humidity was increased, a yellow color appeared in all the films that contained phosphate groups. PU1, the control latex with no Sipomer PAM 200 was still colorless.

As a result of the apparently good formation of the protective phosphatization layer, another corrosion test was carried out in the new coatings, as presented in **Figure 11**.

As observed, very different results are obtained this time. During the first 7.5 h, there is no evidence of corrosion, not even in the area with the defect for none of the coatings, including PU1. After 24 h of exposure to the NaCl solution, the results of PU1 and PU4 did not significantly change with the drying conditions (compared to Figure 8). In PU1, once again, the area with the defect is corroded, while the one without defect is not. In the case of PU4 both areas are corroded. There is, however, a significant improvement on the anticorrosive protection for PU2 and PU3. As observed in Figure 11, even after 24 h of exposure to the NaCl solution, the only rust that is formed is in the uncoated scratch of the defect, but it was not able to propagate further, showing the anticorrosive capacity of these coatings.

This shows that the formation of the iron phosphate does indeed improve the corrosion resistance of waterborne coatings, but that the drying conditions to achieve said passivation layer are not universal. Moreover, the improved performance of PU2 and PU3 with respect to PU4 could be related to a better incorporation of the Sipomer PAM 200 into the particles due to the semibatch feeding of the monomers.
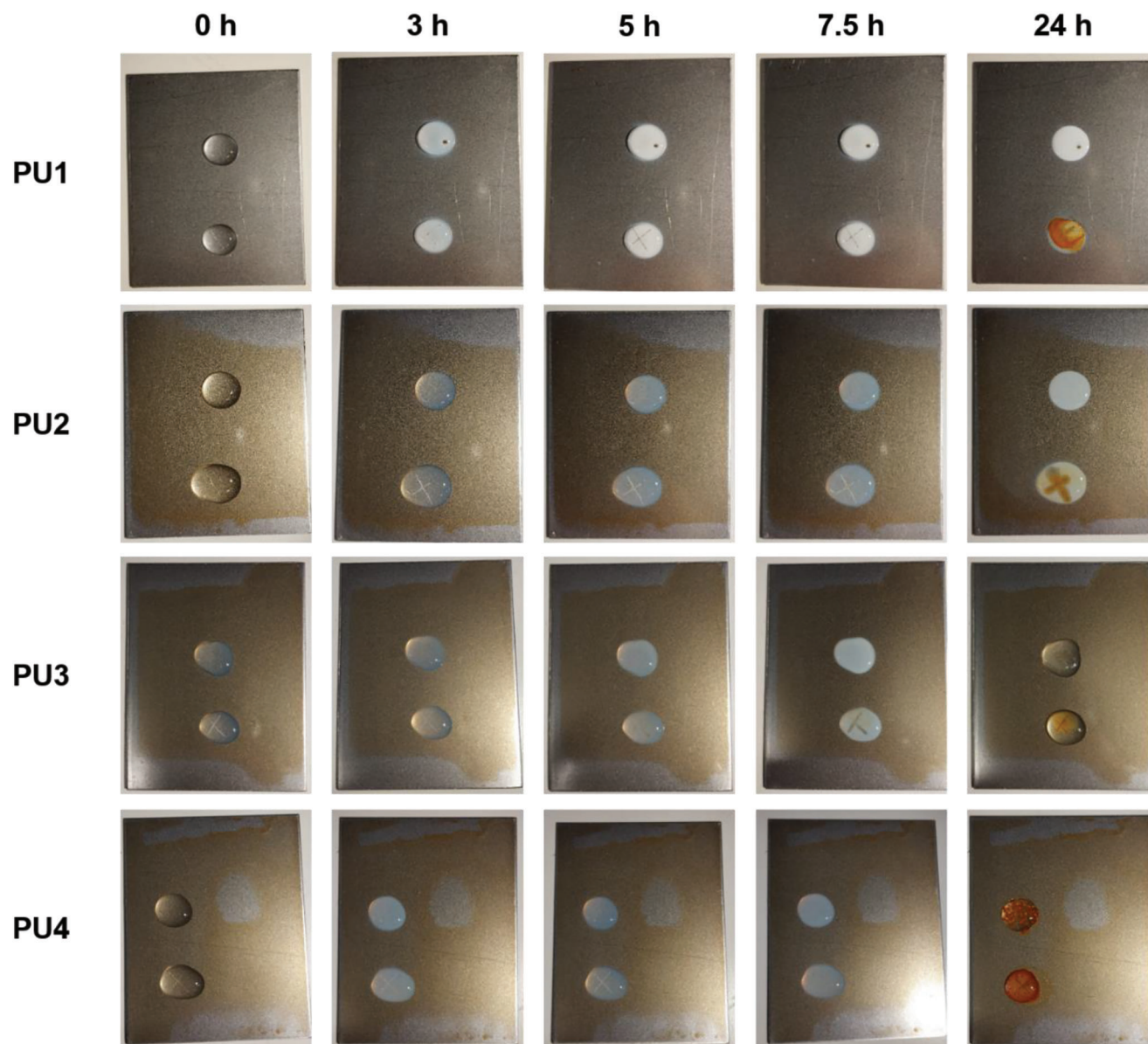
Considering that the coatings obtained after drying at 85% of R.H. show better corrosion resistances than the ones dried at 60% R.H., EIS measurements were done during immersion in 3.5 wt% NaCl aqueous solution. To summarize, **Figure 12** only presents the results of Bode plots (on top) and phase angle diagrams (on the bottom) of specimens after 1 h (left) and 24 h (right) of immersion. Substrates coated with the different polyurethane-acrylic hybrids and bare steel itself (without any coating) are presented for comparison purposes.

In an EIS experiment, the phase angle has a maximum that coincides with the inflection point of a drop in impedance modulus that can be seen on the Bode plot, where the higher the impedance values at low frequency rates, the better the protection of the coating against corrosion. Thus, as expected, all the coated specimens shows higher impedance values than the bare steel sample.

Comparing different samples at 1 h of exposure to NaCl solution, it can be observed that the sample coated with PU2 exhibits good protective behavior. The lowest impedance modulus was obtained for PU1, which can be explained because that is the control latex with no Sipomer PAM200 in the formulation. The impedance values of PU3 and PU4 are in between, showing that some corrosion protection is achieved (compared to PU1), but that the incorporation strategy of Sipomer PAM 200 was more effective in PU2. The results obtained at 24 h of exposure are very similar to the 1 h, as an indication that the coatings did not lose their anticorrosion capacity in this timeframe.

The phase angle of PU2, PU3, and PU4 coatings is higher than 80° at high frequencies and comparing the performance at 24 h of immersion with 1 h, the phase angle remains constant, which means that after the permeation of the electrolyte, the coating capacitance remains relatively stable and the coating system maintains the corrosion protection.

The EIS results are in good agreement with the results obtained for the corrosion test (Figure 11). In the corrosion resistance test, it was not possible to distinguish the performance of PU2 and PU3, but according to the EIS measurement, PU2 gives a better anticorrosion protection. The only outlier of this trend is

**ADVANCED
SCIENCE NEWS**

www.advancedsciencenews.com

{M} acro-
molecular
Reaction Engineering

www.mre-journal.de

Figure 11. Time evolution of the coated steel substrates dried at 23 °C and 85% R.H.: during the corrosion test.

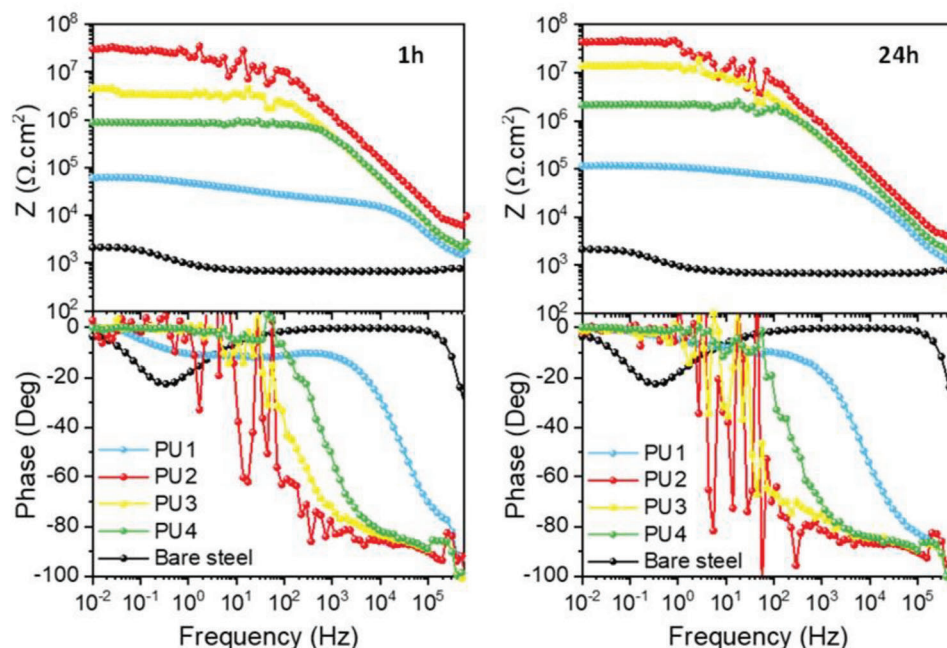PU4, which shows the worst behavior in the corrosion test, while it performs better tan PU1 in the EIS.

4. Conclusions

In this work, we have explored different alternatives to synthetize polyurethane/acrylic hybrid waterborne dispersions that contained phosphate functionality aimed for anticorrosion applications.

It was found that the incorporation of phosphate groups in the PU prepolymer formation was more challenging than expected. Although none of the strategies that we tried could yield a satisfactory hybrid dispersion, some show some promising results that could produce polyurethane-acrylic hybrids with excellent anticorrosive properties with further development.

The second route was much more fruitful. Hybrid latexes were successfully synthetized in a solvent-free method that used the acrylic monomers as solvent for the PU prepolymer, and a second step of free-radical polymerization of the acrylics. It was observed that the addition of Sipomer PAM 200, a phosphate containing monomer, did not alter the latex characteristics nor the water resistance of the film.

The anticorrosive performance of these coatings strongly depended on the drying conditions of the film. When the drying conditions were 23 °C and 60% R.H., the results were underwhelming. Visual observation already suggested that the protective iron phosphate layer was nor formed, and it was confirmed by the different corrosion test. The situation was completely different when the drying conditions were 23 °C and 85% R.H. though. In this case, the characteristic yellow stain of the iron phosphate

ADVANCED
SCIENCE NEWS
www.advancedsciencenews.com

[M]acro-
molecular
Reaction Engineering
www.mre-journal.de

Figure 12. Bode plots (top) and phase angle diagrams (bottom) of EIS measurement for coated steel substrates dried at 23 °C and 85% R.H. after 1 h (left) and 24 h (right) of immersion in 3.5 wt% NaCl aqueous solution.

was clearly visible, and excellent anticorrosive properties were achieved.

Supporting Information

Supporting Information is available from the Wiley Online Library or from the author.

Conflict of Interest

The authors declare no conflict of interest.

Data Availability Statement

The data that support the findings of this study are available from the corresponding author upon reasonable request.

[1] K. Gerhardus, J. Varney, N. Thompson, O. Moghissi, M. Gould, J. Payer, *International Measures of Prevention, Application, and Economics of Corrosion Technologies Study*, NACE Int, Houston, TX **2016**.
[2] M. A. Jafar Mazumder, *Glob. J. Eng. Sci.* **2020**, *5*, 1.
[3] R. Javaherdashti, *Anti-Corrosion Methods Mater.* **2000**, *47*, 34.
[4] Z. Ahmad, *Principles of Corrosion Engineering and Corrosion Control*, Elsevier, New York **2006**. https://doi.org/10.1016/B978-0-7506-5924-6.X5000-4
[5] S. Harsimran, K. Santosh, K. Rakesh, *Proc. Eng. Sci.* **2021**, *3*, 13
[6] B. N. Popov, *Corrosion Engineering: Principles and Solved Problems*, Elsevier, New York **2015**.
[7] S. Lyon, *Science and Technology. In Nuclear Corrosion Science and Engineering*, Elsevier, New York **2012**.
[8] M. F. Montemor, *Surf. Coat. Technol.* **2014**, *258*, 17.
[9] S. B. Lyon, R. Bingham, D. J. Mills, *Prog. Org. Coatings.* **2017**, *102*, 2.
[10] M. Faccini, L Bautista, L. Soldi, A. M. Escobar, M. Altavilla, M. Calvet, A. Dom, E. Dom, *Appl. Sci.* **2021**, *11*, 3446.
[11] C. Jiao, L. Sun, Q. Shao, J. Song, Q. Hu, N. Naik, Z. Guo, *ACS Omega* **2021**, *6*, 2443
[12] F. Sbardella, L. Pronti, M. Santarelli, J. Asua Gonzàlez, M. Bracciale, *Coatings* **2018**, *8*, 283
[13] S. Bilgin, S. Bahraeian, M. L. Liew, R. Tomovska, J. M. Asua, *Prog. Org. Coatings* **2022**, *162*, 106591
[14] S. M. Dron, M. Paulis, *Polymers* **2020**, *12*, 2500.
[15] E. Kientz, Y. Holl, *Colloids Surf., A* **1993**, *78*, 255.
[16] Z. Aguirreurreta, J.-A. Dimmer, I. Willerich, J. R. Leiza, J. C. De La Cal, *Int. J. Adhes. Adhes.* **2016**, *70*, 287
[17] A. Momber, *Mater. Corros.* **2012**, *63*, 404.
[18] J. L. Oliveira, A. W. B. Skilbred, A. Loken, R. R. Henriques, B. G. Soares, *Prog. Org. Coatings* **2021**, *159*, 106387.
[19] M. Khanzadeh Moradllo, M. Shekarchi, M. Hoseini, *Constr. Build. Mater.* **2012**, *30*, 198
[20] E. Armelin, R. Oliver, F. Liesa, J. I. Iribarren, F. Estrany, C. Alemán, *Prog. Org. Coatings* **2007**, *59*, 46.

**ADVANCED
SCIENCE NEWS**

www.advancedsciencenews.com

Ⓜ **acro-
olecular**
Reaction Engineering

www.mre-journal.de

[21] X. Ge, W. Fan, H. Tang, J. Yang, R. Ding, X. Zhao, *Prog. Org. Coatings* **2022**, *174*, 107294.

[22] C. Wang, F. Chu, C. Graillat, A. Guyot, C. Gauthier, J. P. Chapel, *Polymer* **2005**, *46*, 1113.

[23] C.-Y. Li, W.-Y. Chiu, T.-M. Don, *J. Polym. Sci., Part A: Polym. Chem.* **2007**, *45*, 3359.

[24] J. Shao, C. Yu, F. Bian, Y. Zeng, F. Zhang, *ACS Omega.* **2019**, *4*, 2493.

[25] U. Sebenik, M. Krajnc, *J. Polym. Sci., Part A Polym. Chem.* **2005**, *43*, 4050.

[26] A. Lopez, Y. Reyes, E. Degrandi-Contraires, E. Canetta, C. Creton, J. L. Keddie, J. M. Asua, *Macromol. Mater. Eng.* **2013**, *298*, 53.

[27] A. Lopez, E. Degrandi, E. Canetta, J. L. Keddie, C. Creton, J. M. Asua, *Polymer* **2011**, *52*, 3021.

[28] S. Mehravar, N. Ballard, R. Tomovska, J. M. Asua, *Ind. Eng. Chem. Res.* **2019**, *58*, 20902.

[29] S. Mehravar, N. Ballard, A. Veloso, R. Tomovska, J. M. Asua, *Langmuir* **2018**, *34*, 11772.

[30] D. K. Kakati, M. H. George, *Polymer* **1993**, *34*, 4319.

[31] K. Mequanint, R. D. Sanderson, *EP 922736*, **1999**.

[32] K. Mequanint, R. Sanderson, H. Pasch, *Polymer* **2002**, *43*, 5341.

[33] K. Mequanint, R. Sanderson, *Polymer* **2003**, *44*, 2631.

[34] S. Chimenti, J. M. Vega, E. G. Lecina, H.-J. Grande, M. Paulis, J. R. Leiza, *Ind. Eng. Chem. Res.* **2019**, *58*, 21022.

[35] J. M. Vega, S. Chimenti, E. García-Lecina, H.-J. Grande, M. Paulis, J. R. Leiza, *Prog. Org. Coatings* **2019**, *148*, 105706.

[36] S. Chimenti, J. M. Vega, E. García-Lecina, H.-J. Grande, M. Paulis, J. R. Leiza, *React. Funct. Polym.* **2019**, *143*, 104334.

[37] Z. Aguirreurreta, J. C. De La Cal, J. R. Leiza, *Prog. Org. Coatings* **2017**, *112*, 200.

[38] Z. Aguirreurreta, J.-A. Dimmer, I. Willerich, J. C. De La Cal, J. R. Leiza, *Macromol. Mater. Eng.* **2015**, *300*, 925.

[39] R. Kumar, N. Lebedinski, *WO2013138438*, **2013**.

[40] C. H. Bamford, E. F. T. White, *Trans. Faraday Soc.* **1956**, *52*, 716.

[41] S. Chimenti, J. M. Vega, M. Paulis, J. R. Leiza, *Colloid Polym. Sci.* **2022**, *300*, 429.

2300015 (13 of 13)